I CIMMEC
1ST INTERNATIONAL CONGRESS ON MECHANICAL METROLOGY
October, 08 – 10, 2008, Rio de Janeiro, Brazil

DYNAMIC-WEIGHING LIQUID FLOW MEASUREMENTS A DESCRIPTION OF THE MEASUREMENT PROCESS

Jesús Aguilera, Rainer Engel, Gudrun Wendt

PTB Physikalisch-Technische Bundesanstalt, Braunschweig, Germany
jesus.aguilera@ptb.de, rainer.engel@ptb.de, gudrun.wendt@ptb.de

Abstract: The *PTB Liquid Flow Group* is developing a new primary measurement principle to determine liquid flow. Such a measurement principle is based on a dynamic-weighing approach [1], which is able to reproduce the unit of mass flow as a real measurand and not as a difference quotient of mass and time. The measurement concept relies on a mass-spring-damper model that simulates the mechanical response of the dynamic-weighing system (DWS) at different fluid flow conditions. The design and scope of a DWS prototype is also described in this document as well as the experiments that were made, to physically explain the system response.

Keywords: Liquid flow, dynamic weighing, fluid force, mass-spring-damper system

1. INTRODUCTION

At present, the majority of liquid flow primary standards operate under the static-weighing principle with a flying start and finish [2], which yields low measurement uncertainty levels, and it is generally accepted. On the other side, there is a growing interest and demand from the industry to implement a dynamic primary standard that is able to characterize the performance of flowmeters under dynamic conditions, mainly with those metering devices that are involved in the control process of fluids and have a direct impact on any process output and on the economy.

One of the advantages of implementing this new option is that a static-weighing system enhanced by suitable auxiliary devices and a (synchronous) real-time data acquisition system (DAQ) can serve as a dynamic one as well, without changes in its mechanical design.

The main tasks that have been carried out during this ongoing research work are: the functional description of the measuring principle and its differences in relation to the static-weighing system, the design of the DWS prototype, the set up of experiments to analyze the system dynamics, and their results. A system-response comparison between a numerical DWS model and the DWS prototype was also performed, with the aim to derive an equation that best describes the measurement process.

2. DESCRIPTION OF THE MEASUREMENT PROCESS

As a starting point of this research, it must be stated that the *input signal* of the measurement process is the entering liquid mass m_W, which is collected in a vessel during a time t. This statement either applies for a static-weighing system (SWS) or the proposed dynamic-weighing system (DWS).

As for the input signal function of the DWS, it can be agreed that it approximately follows the path of a *ramp function* (**Eq. 1**) during the filling process. This argument is true as long as the system is able to keep a steady liquid flow rate and small transient flows are disregarded.

$$m_W(t) = \int \dot{m}_W \cdot dt \qquad (1)$$

Here, $\dot{m}_W$ stands for a coefficient defining the ramp slope (*mass flow*).

Weighing system

As previously mentioned, the DWS will be implemented upon the mechanical design of the static-weighing system (**Fig. 1**). For this reason, it is worth recalling some aspects of the SWS system, so as to understand how a dynamic mass flow measurement is obtained, and which are the differences between the two measurement principles.

A SWS is essentially a vessel and stop-watch system [2], in which the fluid flow is directed into a collection tank during a period of time T (**Fig. 2**). The change in mass is divided by the collection time to yield the mass flow as shown in a general form in **Eq. 2**:

$$\bar{\dot{m}} = \frac{m_{W,SWS}}{T_{SWS}} \qquad (2)$$

The main components of the SWS applied to measure mass flow rate are: a force transducer (*electromagnetic-force-compensation cell,* EFC), which is used as a weighing

system for this particular research, a collection tank, a connecting pipe where the meter under calibration (MUC) is located, and a diverter valve that bypasses the fluid mass either to the collection tank for effects of measurement or to the supply tank when the collection is completed.

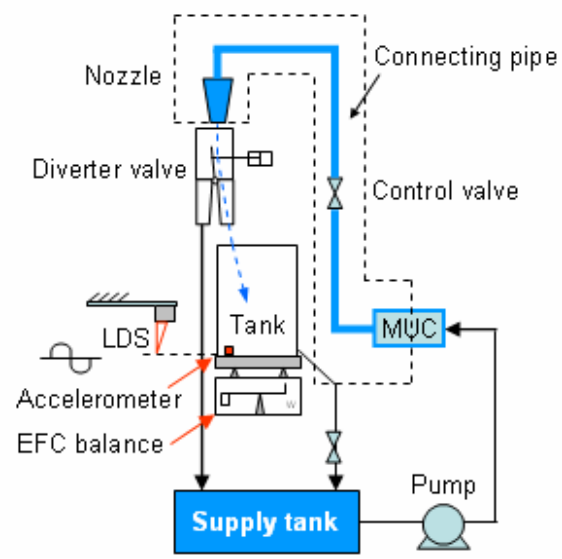

Fig.1 Schematic diagram of an EFC balance and auxiliary devices (LDS and accelerometers) used as a dynamic-weighing system (DWS)

The DWS, illustrated in **Fig. 1,** features all the SWS components described above, in addition to auxiliary devices that monitor the system acceleration (accelerometer), its displacement (laser displacement sensor, LDS), and a real-time data acquisition system.

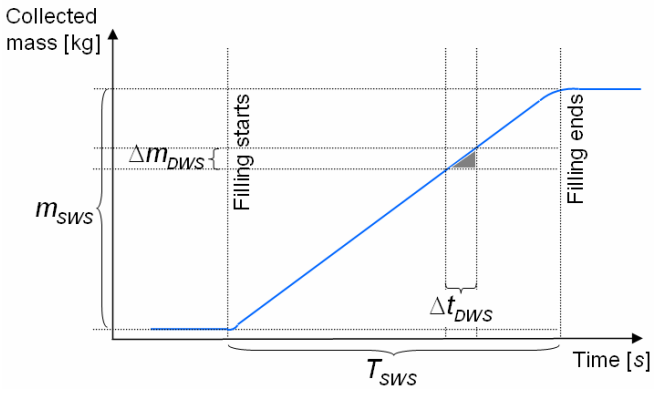

Fig. 2 Graphical representation of the static and dynamic weighing measurement principle

The aim of using the auxiliary variables of displacement and acceleration is to measure the collected liquid mass $\boldsymbol{m_W(t)}$ in reference to the dynamic-weighing principle described in **Eq. 3**. Such a differential equation of motion is an analogous representation of the physical weighing system in terms of a spring, a viscous damper (defining the elastic properties of the EFC sensing element), and a total mass $\boldsymbol{m_T}$ that comprises the supported mass of the DWS , $\boldsymbol{m_{DWS}}$, and the collected liquid as a function of time $\boldsymbol{m_W(t)}$.

Moreover, the system is subjected to a time-varying *fluid force* $\boldsymbol{F_T}$, which is a product of the continuous increment of collected liquid mass (*hydrostatic force,* $\boldsymbol{F_S}$) and the *hydrodynamic force* $\boldsymbol{F_D}$ caused by the impacting water jet against the tank base or water surface.

The system elastic properties of stiffness (***k***) and damping (***c***) have to be characterized in order to match the system response of the DWS. For practical purposes, the system mass is restricted to a translational motion in the direction of weighing (z-axis), whereby the DWS model is defined as a 1-degree-of-freedom (DoF) system represented in **Eq. 3** and illustrated in **Fig. 3**.

$$\left(m_{DWS} + m_W(t)\right)\cdot \ddot{z} + c\cdot \dot{z} + k\cdot z = \left(F_S + F_D\right) \qquad (3)$$

Once $\boldsymbol{m_W(t)}$ is determined by **Eq. 3**, the *mass flow rate* $\dot{\boldsymbol{m}}_{\boldsymbol{W}}$ can be defined as:

$$\dot{m}_W = \frac{\Delta m_W}{\Delta t_{DWS}}\Bigg|_{t}^{t+\Delta t_{DWS}} \qquad (4)$$

where $\boldsymbol{T_{DWS}}$ is the time period taken to perform a dynamic measurement as exemplified in **Fig. 2**.

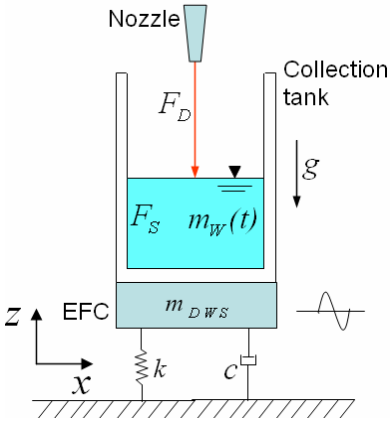

Fig. 3 Spring-damper-mass representation of DWS

An important point to mention is that in reality the DWS is subjected to eccentric and angular fluid forces, whereby the system can respond in 3 to 5 degrees-of-freedom (DoF) [3]. However, the predominant and important system motion for the determination of mass flow is the translational weighing axis (*z-axis*). This statement is a good justification for analyzing the system as a 1-DoF model, as long as an adequate FFT signal analysis is able to separate the harmonics of different motion axes and to identify the eigenfrequency of the weighing axis. Comparison results between the simulated DWS model and the experiments confirm positively such a statement.

Uncertainty contributors

Regarding measurement uncertainty, the main contributor from the static-weighing system is the timing error of the diverter valve. For a DWS system, this contributor turns out to be negligible because DWS measurements are based on continuous flow, and not on the time it takes to collect a certain amount of liquid mass.

Another SWS uncertainty contributor is related to the fact that a liquid flow measurement is a result of an average quasi-steady flow. On the other side, a DWS liquid flow measurement is a product of a continuous-time calculation of mass.

Uncertainty due to evaporation can be very small (or even negligible) in a DWS because of the short time the system needs to calculate mass flow during the filling process. The opposite effect occurs in an SWS that requires a relatively long time to get a stable mass reading from the balance.

The main sources of uncertainty (projected) for the DWS measuring principle are:

- A time-varying magnitude of hydrodynamic force through the filling process, and
- disturbances in the EFC balance readout caused by the internal fluid flow in the tank.

In summary, despite the higher accuracy the static-weighing systems claim, that in relation to the new dynamic principle proposed, the accuracy difference can be compensated by the possibility to characterize the dynamic performance of flowmeters under steady conditions and reduce the calibration time.

3. DWS PROTOTYPE AND EXPERIMENTATION

The DWS prototype shown in **Fig. 1** and **Fig. 4** comprises a source of steady flow, a control valve to set the desired flow rate, a connecting pipe, a liquid flow check standard (turbine flowmeter), a diverter valve (with non-fast actuation required), and a 10-L collection vessel made of glass with the goal to visualize the internal flow and the water-jet penetration depth. The test fluid used in the system is water.

The weighing system is a 30 kg EFC balance with a resolution of 0,1 g, a maximum *data sampling rate of 20 Hz* for this particular application, and a set of signal filters that provides different attenuation levels.

The DWS prototype is capable of performing measurements with different size of glass vessels with the aim to analyze the dimensional and geometrical effects of collection tanks on the DWS response. Furthermore, the location of the nozzle in relation to the balance platform can be shifted in order to see the eccentricity effects on the system output signal. The trajectory of the water-jet can be driven at 90° (in reference to the balance platform) or 95° with the intention to study the system reaction to angular and normal hydrodynamic forces.

The operational flow range of the prototype is from 1 L/min to 10 L/min through a 25-mm-diameter pipeline.

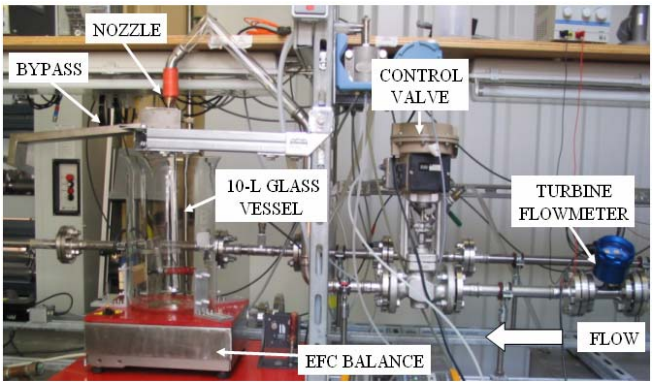

Fig. 4 Dynamic-weighing system used as a prototype (DWS)

Auxiliary devices

A piezoelectric *accelerometer* is mounted on top of the EFC balance platform to measure the *acceleration* of the system upon the weighing axis (z-axis). The transducer measures within a range of $\pm 70\,\mathrm{m/s^2}$, a sensitivity of $106\ \mathrm{mV/(m\cdot s^{-2})}$, and a frequency range of 0,4 Hz to 8 kHz.

The *non-contact laser displacement sensor* (LDS) is installed over the EFC balance to track the weighing system displacement with a resolution of $0{,}5\,\mu m$, and a data sampling rate of 2,5 kHz. This device working under the triangulation measurement principle [4] is an excellent sensor that avoids any undesired force upon the EFC balance.

The *velocity measurement* can be derived from the displacement or acceleration measurements by applying a derivative or an integral, respectively.

The liquid flow check standard employed to set the flow rate during the experiments is a *DN-25 turbine flowmeter*, with a nominal flow range from 1 L/min to 10 L/min.

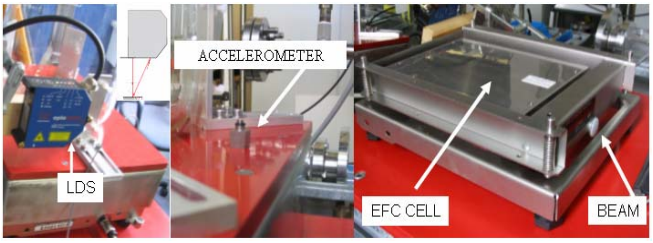

Fig.5 Laser-displacement sensor (LDS), piezoelectric accelerometer, and EFC balance

Data acquisition (DAQ)

The synchronized data acquisition system used for dynamic-weighing measurements is realized by a dedicated

hardware (NI CompactRIO®*), which features an embedded real-time 400-MHz processor, serving as a controller, and customized I/O modules, directly connected to the auxiliary devices [5]. A RS-232 serial port is also available for the interfacing of the EFC precision balance.

The usage of a dedicated hardware enhances the system performance of data logging, real-time signal analysis, and efficient communication to the host computer via high-speed PCI bus. In a few words, the speed of the DAQ system will be only limited by the data sampling rate of the sensors and I/O modules rather than its processing performance. For this application, the maximum *data sampling rate for all acquired signals (except the EFC) is 250 Hz.*

EFC balance and DWS stiffness coefficient (*k*)

Generally, one would state that the EFC balance supporting the collection vessel is designed only to reproduce the unit of water mass. Indeed, this is true; the displayed result is expressed in a mass unit (*kg*). However most of weighing systems do not measure mass directly, but rather force at the moment the water mass is being collected [3].

Electromagnetic-force compensation cells (EFC) fall within this approach as they use the physical principle of force measurement to display mass readings. In this case, the EFC cell uses a scaled factor based on a reference mass and the acceleration of gravity during its calibration to display a magnitude in kilograms [6].

For this application, the measurement of the total hydraulic force will be determined by the EFC balance.

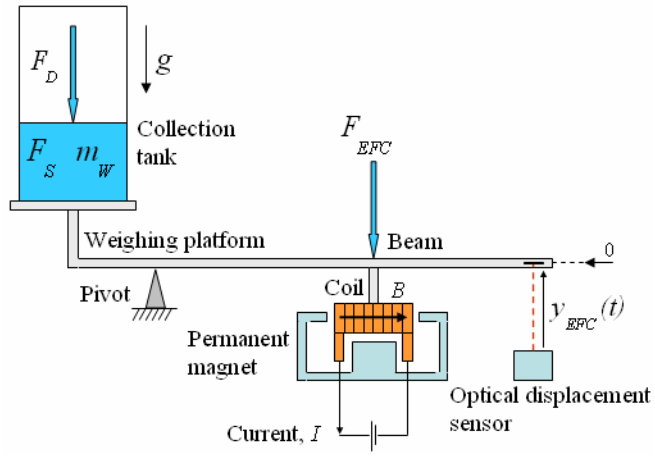

Fig. 6 Diagram of a EFC balance components and its analogous representation

Another interesting analogy is that an EFC balance features mechanical elastic properties of stiffness and damping. As for the stiffness, the cell can be analyzed as an equivalent spring-lever system (See **Fig. 5, Fig. 6** and **Fig. 7**), where the stiffness coefficient ***k*** is strongly related to the EFC response when a force is applied to it. The characterization of the *DWS stiffness coefficient* consists in measuring the displacement of the balance platform caused by an acting reference force: $\boldsymbol{k = F_{Ref} / dz}$.

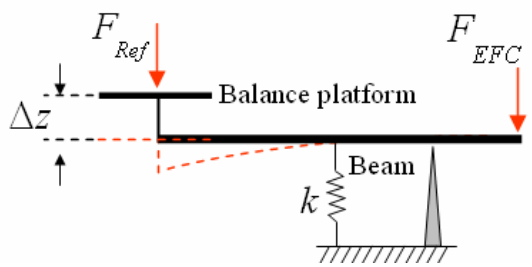

Fig. 7 Spring-lever representation of the EFC balance

An important point to mention is that an EFC balance undergoes a varying stiffness coefficient caused by the induced-electromagnetic compensation force. In the next paragraphs, a brief explanation of the EFC measuring principle is given in order to describe what occurs internally in the balance and how the spring-lever concept is applied.

The EFC balance measures the force applied by the collected water mass and the fluid in motion (input signal) by means of a compensating current. Such a current signal (***I***) flows through a coil (attached to a beam), which is inserted in a permanent magnetic field as illustrated in **Fig. 6**. When a force acts upon the balance, the beam moves from its equilibrium condition [7]. As this happens, an optical positioning sensor monitors the coil position and sends a feedback current signal to immediately return the beam in its zero position (within an accuracy of $1\,\mu m$). In mechanical terms, the zero positioning control loop can be described in its behavior as a proportional change of the spring stiffness in relation to the time-varying force being applied to the balance platform.

The electromagnetic compensation force is depicted as:

$$F_{EFC} = I \cdot B \cdot L \qquad (5)$$

Here, ***I*** stands for current, ***B*** for magnetic flux density in the air gap, and ***L*** for the effective wire length of the coil.

A characterization of the EFC spring coefficient was carried out by applying reference masses placed upon the DWS platform (1 kg, 3 kg, 5 kg, 7 kg, 9 kg and 10 kg) and the acceleration of gravity to calculate the reference force. The balance platform displacement is measured continuously by a laser-displacement sensor (LDS) everytime a load is applied. Thereafter, a force vs. displacement graph is plotted, and a linear regression is applied to the curve in order to get its describing equation.

The derivative of such a curve fitting equation (**Eq. 6**) yields the stiffness coefficient as a function of z:

$$k = \frac{dF(z)}{dz} = 6{,}830 \cdot 10^{8} \cdot z + 4{,}1089 \cdot 10^{5} \qquad (6)$$

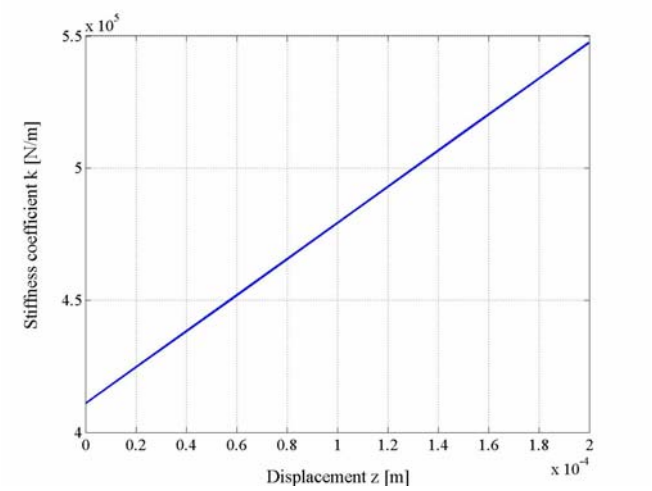

Fig.8 Stiffness coefficient curve as a function of the system displacement

DWS damping coefficient (*c*)

The determination of the EFC damping coefficient at first requires the characterization of the *undamped natural angular frequency* ω_n for the fact that the supported mass upon the system changes through the time. Thus, the undamped natural angular frequency is described by the following equation:

$$\omega_n = \left(\frac{k}{m}\right)^{1/2} \tag{7}$$

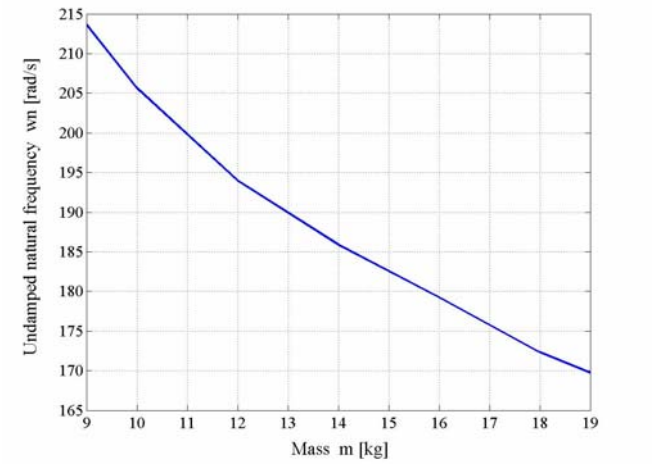

Fig. 9 Undamped natural frequency (ω_n) change as a function of collected water mass (*m*)

The *critical damping coefficient* c_c is another variable which has to be determined in order to know the minimum viscous damping that will allow the system to return to its initial position without oscillation:

$$c_c = 2 \cdot m \cdot \omega_n \tag{8}$$

Once the c_c values have been calculated in terms of ω_n and m, the only variable missing to derive the damping coefficient c is the ratio of the *undamped natural angular frequency* and the *damped angular frequency* ω_d, known as damping ratio ζ.

Thus, the *damping ratio* and the damping coefficient are respectively defined as:

$$\frac{\omega_d}{\omega_n} = (1 - \zeta^2)^{0.5} \tag{9}$$

$$c = \zeta \cdot c_c \tag{10}$$

ω_d is experimentally determined by means of an *FFT analysis* applied to the displacement measurement data taken during the filling process. The main task of the FFT analysis is to find out the frequency spectrum that corresponds to the weighing-axis (z-axis).

The resulting damping coefficient c will provide key information on how quickly the system transfers or dissipates energy (potential energy from the spring and kinetic energy from the mass) through the measurement process.

FFT analysis

The aim of the FFT analysis is to demonstrate that the DWS is indeed a multi-axis system (**Fig. 10**), wherein the system oscillatory motion at any axis can have a *crosstalk effect* on the weighing axis. The multi-axis motion is assumed to be a disturbance. However it is possible to eliminate (or attenuate) from the output signal response by recognizing the eigenfrequencies belonging to each motion axis of the system.

The numerical simulations of the measurement process performed in this investigation confirm that only the motion of the weighing axis is necessary to calculate the mass flow rate based on **Eq. 3** and **Eq. 4**.

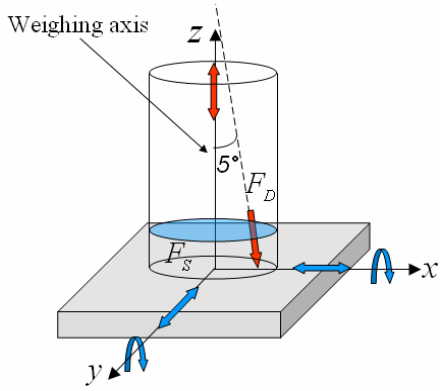

Fig. 10 Degrees of freedom of DWS and acting fluid forces

X-axis

The frequency amplitudes at different system axes shown in **Fig. 11** give an overview of how quickly the system dissipates energy as a function of the collected water mass and the hydrodynamic force. Furthermore, the *crosstalk effect* can be clearly seen at any axis of the DWS

due to the fact that more than one harmonic is present. In total, four harmonics are recognized by the FFT analysis, wherein one of these describes the oscillating frequency of the weighing axis.

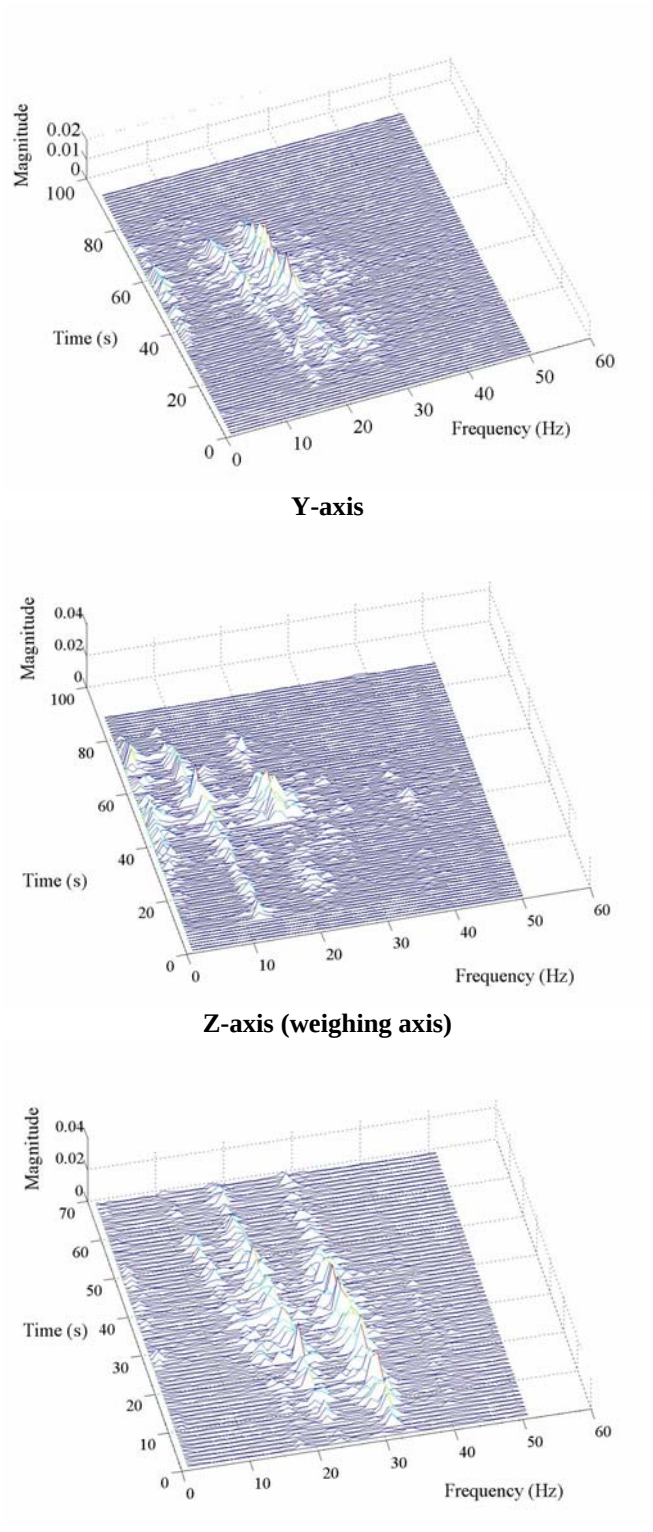

Fig. 11 Waterfall plots showing the DWS non-stationary eigenfrequencies due to continuous water mass increments and fluid-induced forces (*FFT waterfall time period: 1 s*)

The data used for the FFT analysis were acquired by means of the LDS at three different linear axes (x, y and z). The data recording time comprises the whole water collection at a mass flow rate of 8,9 L/min. The water jet impact force (hydrodynamic force) is oriented at 5° with respect to the z-axis with the purpose to amplify the lateral and angular motion of the balance platform. Notice that the angular orientation of the water jet is a common characteristic in most liquid flow standards due to their diverter-valve design. The FFT is performed on 256 data samples, and at a sampling time of 4 ms.

The waterfall graph is a very useful tool that encloses the global dynamics of the DWS, especially, the frequency shift of the system harmonics along the collection time.

As for the results depicted in **Fig. 11**, the eigenfrequencies of the DWS system are non-stationary because the system is subjected to a continuous change of water mass and fluid forces during the filling process.

4. NUMERICAL SIMULATION OF THE DYNAMIC WEIGHING SYSTEM

The numerical simulation of the DWS is an important step to derive the mathematical model that best describes the measurement process (dynamic-weighing), to identify its significant measurement variables for the accurate determination of the measurand (mass flow rate), and to quantify the magnitude of its sensitivity coefficients for a future dynamic-measurement uncertainty analysis.

The numerical model of the system also allows to understand the relation between the system response and the fluid-mechanical interaction. Likewise, the DWS model provides capabilities to test and to manipulate the system input/outputs in a less time-consuming condition rather than in the real system. Additionally, the DWS model offers the possibility of measuring inaccessible variables that in the real system are impossible to be acquired.

For this investigation, the DWS system is simulated according to the geometrical and dimensional characteristics of the DWS prototype at a **constant flow rate** of *8,9 L/min.* The resulting output signals of oscillating frequency, mass, force, and displacement are compared with the attained experimental results at the same nominal flow rate.

Input variable

The variable that governs the numerical simulation is the collected water mass $\boldsymbol{m_W(t)}$, described as an input-signal ramp function, given in **Eq. 1**.

Fluid force

The determination of the fluid force acting upon the weighing system requires a calculation of the time-varying hydrodynamic and hydrostatic forces [3]. Concerning the hydrodynamic force, the water-jet impact height $\boldsymbol{h_i(t)}$ is calculated as a function of the height existing between the nozzle outlet and the tank base (**Fig. 12**), the tank internal

diameter d_T, the collected water mass in the vessel $m_W(t)$, and the water density ρ_w:

$$h_i(t) = h_0 - \left(\frac{4 \cdot m_W(t)}{\rho_w \cdot \pi \cdot d_T^2} \right) \quad (11)$$

The following step is to define the impact velocity of the water jet, taking into account that, for simulation purposes, the water jet velocity vector acts in a normal direction to the tank base (or water surface) and at the center of the balance platform.

According to the Bernoulli equation, *the water-jet impact velocity* u_i is depicted as:

$$u_i(t) = \left[u_n^2 + 2 \cdot g \cdot h_i(t) \right]^{0.5} \quad (12)$$

In order to have all the measurement variables in terms of the input signal, the water-jet velocity variable at the nozzle outlet u_n from **Eq. 12** is substituted in terms of entering water mass by applying the continuity law to the water-jet. Thus, the water-jet impact velocity is re-written in the following form:

$$u_i(t) = \left[\left(\frac{m_W(t)}{\rho_W \cdot A_n \cdot \int dt} \right)^2 + 2 \cdot g \cdot h_i(t) \right]^{0.5} \quad (13)$$

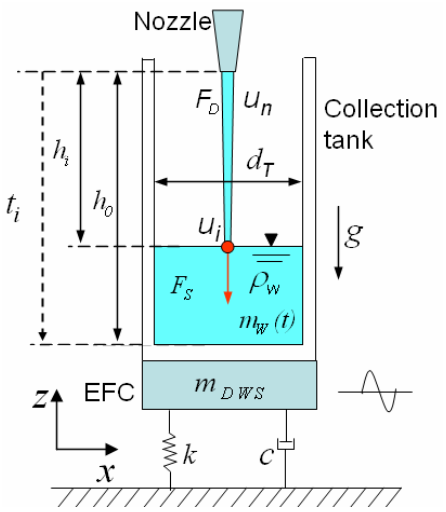

Fig. 12 Description of DWS measurement variables used for the numerical simulation

The hydrodynamic force of the impacting water jet against the tank base (or water surface) is given as:

$$F_D(t) = u_i \cdot \frac{m_W(t)}{\int dt} \quad (14)$$

The water-jet impact time given in **Eq. 15** is an important variable that provides information, not only about the time when filling process starts but it also defines the magnitude of the hydrodynamic and the hydrostatic forces (seen as a water column) at the first impact against the tank base:

$$t_i = \frac{h_i}{u_i} \quad (15)$$

On the other side, the *hydrostatic force* generated by the collected water is:

$$F_S(t) = m_W(t) \cdot g \quad (16)$$

DWS Equation of motion

In order to simulate the DWS output signal at a certain input mass flow rate, the 1-DoF equation of motion is applied (**Eq. 17**). Such a differential equation features the system motion upon the weighing axis with the corresponding elastic properties of the EFC balance.

$$F_T(t) = \left(m_{DWS} + m_W(t) \right) \cdot \frac{d^2 z}{dt^2} + c \cdot \frac{dz}{dt} + k \cdot z(t) \quad (17)$$

In order to attain the time-domain solution of these *input-output equations* (**Eq. 1**, **11**, **13**, **14, 15, 16** and **17**), a *numerical integration algorithm* is implemented to compute the system dynamics over continuous time.

Simulink®* is the numerical integration software used for this task due to its wide number of accurate *numerical solvers* available and its interactive graphical environment that represents the relationship between system variables and coefficients.

The numerical solver employed during the simulation run is the *explicit Runge-Kutta method* [8], with a sampling time of 4 ms and an error tolerance for each time step of 0.1%.

5. RESULTS

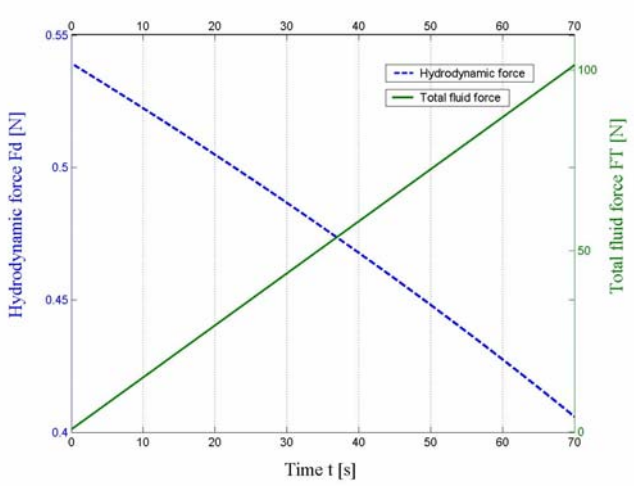

Fig. 13 Simulated time-varying hydrodynamic and total fluid forces at 8,9 L/min

As illustrated in **Fig. 13**, the simulated time-varying hydrodynamic force does decrease along the filling process.

The data presented in **Fig. 14** show a comparison between the EFC balance readout and the simulated water mass collected in the tank. The results reveal that the EFC balance readout is being disturbed by the fluid force.

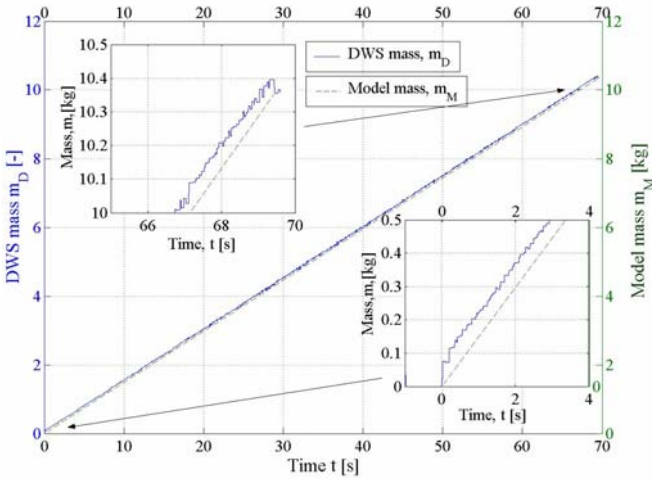

Fig. 14 Comparison between system and model water mass collection

The numerical results of the total fluid force depicted in **Fig. 15** demonstrate that the DWS model accurately follows the total fluid force exerted upon the DWS prototype through the collection time.

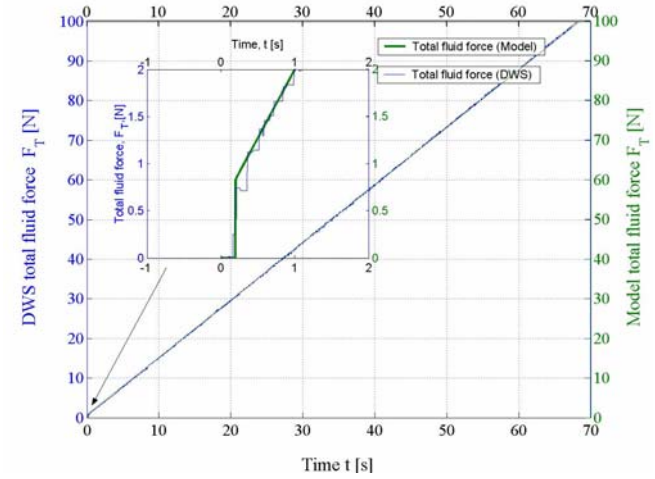

Fig. 15 DWS and model total fluid force response

The DWS and model displacement measurements are also compared in **Fig. 16**. As shown, the simulated displacement signal is within the range of the signal output obtained by the laser displacement sensor. Notice that the noise amplitude is very significant and a second harmonic is present, as it is demonstrated by the FFT analysis (**Fig. 11**) performed on the z-axis (or weighing axis).

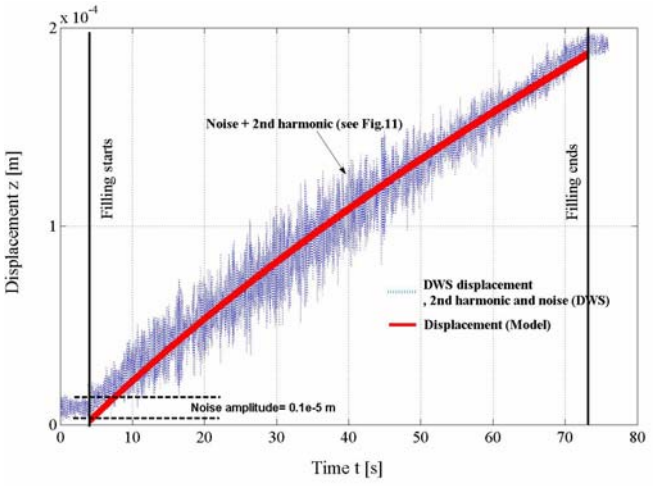

Fig. 16 DWS and model displacement measurements

The DWS and model damped angular frequencies are also compared in **Fig. 17**. The numerical results given do agree very well after the amount of water collected has exceeded 2 kg. The frequency scattering seen at the initial stage of the simulation can be reduced by refining the characterization of the balance stiffness coefficient, and/or applying a more suitable curve fitting regression.

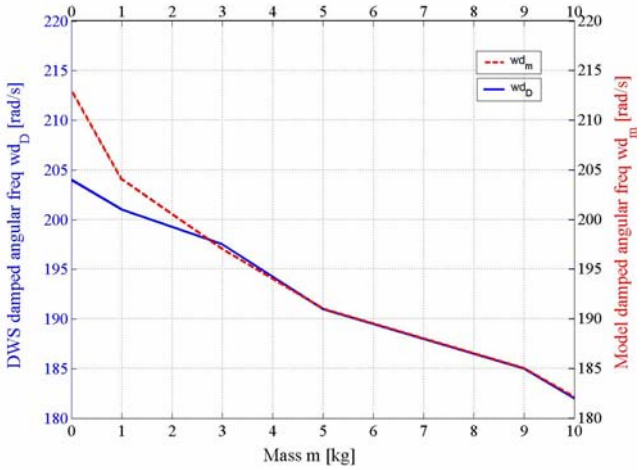

Fig. 17 DWS and model damped angular frequency shift

The damped angular frequency response plotted in **Fig. 17** is one of the two eigenfrequencies found on the z-axis via experimentation (see **Fig. 11**). Such an eigenfrequency coincides with the calculated damped angular frequency. Therefore, this is assumed to be the oscillating frequency of the weighing axis.

The damping coefficient was not applied in the simulation because of the difference in magnitude between the numerical and the experimental damped angular frequency at the first stage of the measurement process (see **Fig. 17** and **Eq. 9**). Such a difference can originate damping coefficient values that cannot be at present validated until more information about the signal response is provided.

** Certain commercial instruments or software are identified in this paper to foster understanding. Such identification does not imply recommendation or endorsement by the PTB, nor does it*

imply that the instruments or software described are necessarily the best available for the application.

6 CONCLUSIONS

- The balance input signal of the accumulated water mass approximately follows a ramp function.
- The hydrodynamic force effects cannot be disregarded from the determination of mass flow rate under dynamic conditions.
- The unit displayed by the balance is the product of a scaled factor given by the manufacturer to convert the quantity force into a mass reading. In the reality, a EFC balance does not measure mass but force.
- The DWS model, presented to describe the measurement process is capable of simulating the dynamic response, within an acceptable degree of accuracy as demonstrated with the comparison results from the experiments.
- The FFT analysis is a powerful tool to identify the frequency spectra that influence the system output signal. After a thorough numerical and experimental analysis, the eigenfrequency belonging to the weighing axis was found.
- It is very important to accurately determine the elastic properties of the DWS (stiffness and damping) in order to have a numerical model that can describe the real measurement process as accurate as needed. Otherwise, the result will yield significant errors and/or a wrong interpretation of the system behavior.
- In the reality the system is subjected to 3 to 5 DoF.
- Continuous improvement on the numerical model and further experimentation are an ongoing task in order to realize which measurement process variables are having the most significant impact on the measurand.

ACKNOWLEDGEMENTS

The authors greatly appreciate the technical support and advices given by Andreas Hein, Klaus Mittelstaedt and Dr. Iryna Marfenko during the prototype construction, experiments, and data analysis performed during this research work.

REFERENCES

[1] R. Engel, "Dynamic-weighing – Improvements in gravimetric liquid flowmeter calibration", 5th ISFFM, Arlington, VA,USA,2002

[2] ISO 9368-1:1990, "Measurement of liquid flow in closed conduits by the weighing method –Procedures for checking installations- Part 1: Static weighing systems", Switzerland, 1990

[3] J. Aguilera, R. Engel, G. Wendt, "Dynamic-weighing liquid flow calibration system –Realization of a model-based concept", FLOMEKO 2007, Johannesburg, South Africa, September 18-21, 2007

[4] L. Stenberg, "Designing a triangulation probe", The SiTek PSD-school, München, Germany, 1995

[5] National Instruments™, "NI compactRIO – Reconfigurable control and automation system",USA, 2006

[6] A. Reichmuth, "Measuring mass and force with a balance", Mettler Toledo AG, Greifensee, Switzerland, 1999

[7] D. Reber, "Electromagnetic force compensation devices in mass comparators", Mettler Toledo AG Greifensee, Switzerland, 2000

[8] The Mathworks inc., "Simulink® Dynamic system simulation for MATLAB®", Version 3, Natick, MA, USA, 1999